# PPIG: Productive and Pathogenic Image Generation for Plant Disease Diagnosis

Satoi Kanno*, Shunta Nagasawa*, Quan Huu Cap*, Syogo Shibuya*,
Hiroyuki Uga†, Satoshi Kagiwada‡ and Hitoshi Iyatomi*

* Applied Informatics, Graduate School of Science and Engineering, Hosei University, Tokyo, Japan
{satoi.kanno.2r@stu., shunta.nagasawa.2u@stu., huu.quan.cap.78@stu.,
syogo.shibuya.5u@stu., iyatomi@}hosei.ac.jp
† Saitama Agricultural Technology Research Center, Saitama, Japan
uga.hiroyuki@pref.saitama.lg.jp
‡ Clinical Plant Science, Faculty of Bioscience and Applied Chemistry, Hosei University, Tokyo, Japan
kagiwada@hosei.ac.jp

*Abstract*—Image-based autonomous diagnosis for plants is a difficult task since plant symptoms are visually subtle. This subtlety leads to the system overfitting as it sometimes responds to non-essential parts in images such as background or sunlight conditions. Thus, this causes a significant drop in performance when diagnosing diseases in different test fields. Several data augmentation methods utilizing generative adversarial networks (GANs) have been proposed to address this overfitting problem. However, performance improvement is limited due to the limited variety of generated images. This study proposes a productive and pathogenic image generation (PPIG) technique, a framework for generating varied and quality plant images to train the diagnostic systems. PPIG is comprised of two phases: the bulk production phase and the pathogenic phase. In the first phase, a number of healthy leaf images are generated to form the basis for the generation of disease images. Then, in the second phase, the symptomatic characteristics are added to the leaf part of the generated healthy images. In this study, we conducted experiments to evaluate PPIG using test images taken in different fields from the training images, assuming six disease classes of cucumber leaves. The proposed PPIG can generate natural-looking, healthy and disease images, and data augmentation using these images effectively improved the robustness of the diagnostic system. Experiments on 8,834 test images taken in different fields from 53,045 training images show that our proposal improved the disease diagnostic performance from the baseline by 9.4% for the macro-average F1-score. Moreover, it also outperformed the previous cutting-edge data augmentation methodology by 4.5%.

*Index Terms*—data augmentation, plant disease diagnosis, generative adversarial networks, image processing, deep learning.

## I. INTRODUCTION

Plant diseases cause lower yields and a decline in the value of agricultural commodities. It is estimated that more than 40% of the world's food crop is lost due to plant pests and diseases [1]. Therefore, early detection of diseases for appropriate measures such as applying pesticides and thinning plants is required. However, the current diagnosis of plant diseases is usually based on visual observation by experts and, if necessary, genetic testing at a specialized institution, which is costly in terms of human, finance, and time.

For this reason, the development of inexpensive automated systems for plant disease diagnosis using machine learning has been carried out. In 2015, one of the first developments of an automatic disease diagnosis system using deep learning technology for cucumber leaf images taken in the field was proposed [2]. Since then, with the rapid spread of deep learning technology and the popularity of PlantVillage dataset [3], a large-scale open dataset of plant diseases, many deep learning-based diagnostic systems have been proposed one after another, and have achieved very good classification performance [4]–[7]. However, at the time, the leaf images from this dataset were pre-cropped and placed on a plain background. Therefore, a significant drop in the classification ability has been reported due to the dissimilarity between the characteristics of the input images in a practical environment and the images in the dataset [4], [8].

For practicality, studies using images taken in actual fields [7], [9] have become the mainstream, and they have reported excellent diagnostic performances. Studies using object detection models such as Faster R-CNN [10] and single shot multibox detector (SSD) [11] have also been carried out to detect disease areas in slightly wide-angle images of many objects, such as leaves in actual fields [12]–[15]. However, most of these conventional studies conflate groups of images were taken and divide them into training and test data for evaluation, resulting in evaluation with images with similar conditions (i.e., background, angle, sunlight exposure, etc.) to the images included in the training data. Thus, the "latent similarity" between training and test data could lead to the model overfitting. We have recently pointed out from our large scale and multi-site experiments that the classification performance is significantly reduced when tests from completely different locations than the training data [13], [14], [16]. We believe that the cause of model overfitting is largely attributed to the similarity of background between the datasets. This could be a distraction that makes the model sometimes respond to the background rather than target leaf areas [16], [17].

One way to reduce this problem is to enrich the diversity of image backgrounds of the training data. However, it is not that

easy to collect sufficient variety of disease data for training in practice. Recently, a few data augmentation (DA) methods using generative adversarial networks (GANs) [18] for automated plant disease diagnosis have been proposed [19]–[22]. All of those methods were designed based on the deep convolutional generative adversarial networks (DCGAN) [23] to directly generate more training data from noise. Although they showed a promising approach, they are not reliable in practice usage since they trained their methods using the PlantVillage dataset [3]. As we mentioned earlier, each leaf image in that dataset has an uniform background, and thus, the variety of generated backgrounds has no improvement.

More studies on DA for practical in-field images diagnosis using an image-to-image transformation method so-called CycleGAN [24] that performs unsupervised domains transformation have also been utilized [25], [26]. Those studies applied CycleGAN to generate diseased leaf image from healthy data thanks to their sophisticated style transformation function. However, since CycleGAN transforms the entire image, the generated images quality are not satisfactory because the appropriate areas to be given disease signs are not taken into account, and unexpected changes are made to the background. In addition, the distribution corresponding to the image generated by this method is considered to be a interpolated point in the domain of the generated image. Therefore, the effect of applying these generated images as DA is limited.

To solve that problem, Cap et al. proposed an improved version of CycleGAN called LeafGAN to transform healthy cucumber leaf images to diseases [27]. LeafGAN applies the transformation to only the leaf region using background segmentation masks produced from a weakly supervised learning method. Therefore, the background information of the healthy image can be kept in the transformed image, and thus the quality of the generated images is much better than the originals and their distribution is different from either the original healthy or diseased domain. But since LeafGAN is a one-to-one corresponding image transformation model, the number of generated images highly depends on the number of base healthy images.

We hypothesize that if we could generate a larger number of healthy images, we could increase the diversity of generated disease images, which could be used as an effective DA process. In this study, we propose productive and pathogenic image generation (PPIG) - a two-phase noise-to-image generation method that addresses the lack of image diversity problem. The main idea of the proposed PPIG is to first generate several healthy images from noise as a base image from which the features of the disease will be transferred (bulk production phase). The disease symptoms are then transferred to the region of interest (i.e., leaf region) of the large number of healthy images generated in the former phase using an image-to-image transformation models (pathogenic phase).

With this approach, we can use the PPIG as a useful DA technique and generate an infinite number of disease images with much more diversity. We observe that our proposal not only produces natural and diverse images but also helps
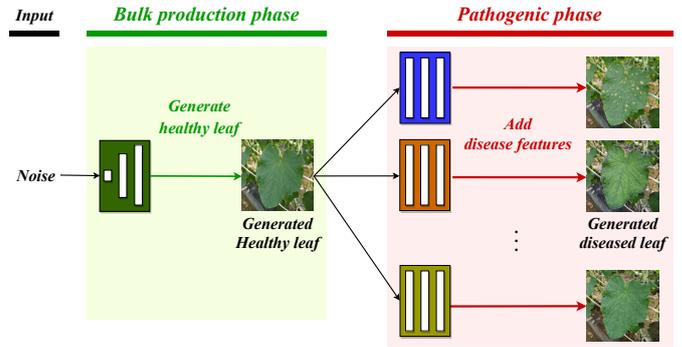


Fig. 1. A number of healthy images are generated during the bulk generation phase, each of which is transformed into a disease image during the pathogenic phase

boosting the disease diagnostic performance on unseen test data by using the generated images as training resources.

## II. METHOD

In this study, we propose a two-phase method for generating diverse and massive images using two different GANs methods. Fig. 1 shows an overview of our system. Our method can generate a wide variety of images for fine-grained classes (i.e., diseased leaves). We use the method as a DA technique to improve the discrimination performance.

The proposed PPIG consists of two phases: (1) bulk production phase and (2) pathogenic phase. In the first phase, realistic healthy leaf images are generated from noise using styleGAN2 [28], which is the state-of-the-art GANs method for generating high-definition images. In the second phase, we use models that has been trained to transform healthy $\leftrightarrow$ diseases and add disease characteristics to the real or generated healthy leaf images. These phases make it possible to obtain many diseased leaf images from various healthy images generated without restrictions.

### A. Bulk production phase

In the diagnostic problem of plant diseases occurring on leaves, analysis of the leaf region in the image is essential. Diseased leaves change from their original healthy leaf state. Therefore, this phase produces high-resolution images of healthy leaves with no disease signs as inputs for the second phase.

In this study, the generation was performed using styleGAN2 [28] which is a state-of-the-art GANs-based image generator that can generate high-definition images. This phase's input is a noise vector, and the output is a generated pseudo healthy image.

### B. Pathogenic phase

In this phase, we add disease characteristics to the leaf region in images of various pseudo-healthy leaves generated in the previous process to realize "disease initiation processing."

*1) General outline:* To realize the function of this phase, disease transformation models based on LeafGAN [27], a modified version of CycleGAN for automatic plant disease diagnosis, are used. LeafGAN is a method for generating images by adding symptoms only to the leaf region. This method not only improves the image quality but also adds images generated, as DA was effective in training the disease classifier. The disease transformation model needs to obtain background mask images for training. While the original Leaf-GAN uses masks acquired by a weakly supervised learning for leaf region extraction, in this study, we applied a supervised method called anti-overfitting pre-treatment (AOP) [16], which is based on pix2pix [29] and provides more accurate leaf region segmentation. AOP is reported to have successfully isolated cucumber leaf images from the background automatically with an F1-score of 98.1% by supervised learning using 8,000 segmentation mask images.

*2) Formulaic explanation:* In our experiments, the previous AOP model trained on 8,000 cucumber leaf images was also used for leaf region extraction. The leaf images $x \in X$ and $y \in Y$ are fed into the trained AOP model, and the output were background masking images $S_x$ and $S_y$, with healthy and disease domains are expressed as X and Y.

Similar to LeafGAN, disease transformation models used in this phase have two generators ($G : X \rightarrow Y$ and $F : Y \rightarrow X$) and two discriminators ($D_X$, $D_Y$) to perform domains transformation. In training $G$, discriminator $D_Y$ identifies whether the generated image $x' = G(x)$ is a real image $y_i \in Y$ or not. The mapping $F$ and the corresponding discriminator $D_X$ learns to discriminate the generated image $y' = F(y)$ from the real image $x_i \in X$ simultaneously.

In the training of $G$, the adversarial loss in $G : X \rightarrow Y$ is as follows.

$$\mathcal{L}_{\mathrm{adv}}(G, D_Y) = \mathbb{E}_{y \sim p_{\mathrm{data}}(y)}\big[\big(D_Y(y_s) - 1\big)^2\big] \\ + \mathbb{E}_{x \sim p_{data}(x)}\big[\big(D_Y(x'_s)\big)^2\big]. \quad (1)$$

where $x'_s = S_x \odot x'$, $y'_s = S_y \odot y'$ and $x_s = S_x \odot x$, $y_s = S_y \odot y$ are masked $x \in X$, $y \in Y$.

Similarly, the adversarial loss for $F : Y \rightarrow X$ is as follows:

$$\mathcal{L}_{\mathrm{adv}}(F, D_X) = \mathbb{E}_{x \sim p_{\mathrm{data}}(x)}\big[\big(D_X(x_s) - 1\big)^2\big] \\ + \mathbb{E}_{y \sim p_{\mathrm{data}}(y)}\big[\big(D_X(y'_s)\big)^2\big]. \quad (2)$$

The cycle consistency loss that keeps the two domains consistent is as follows:

$$\mathcal{L}_{\mathrm{cyc}}(G, F) = \mathbb{E}_{x \sim p_{data}(x)}\big[|F(G(x)) - x|_1\big] \\ + \mathbb{E}_{y \sim p_{\mathrm{data}}(y)}\big[|G(F(y)) - y|_1\big]. \quad (3)$$

LeafGAN introduces a background similarity loss, $\mathcal{L}_{\mathrm{bs}}$, in order to keep the backgrounds of generated images as similar as original images. $\mathcal{L}_{\mathrm{bs}}$ is a term for minimizing the L1 distance of the background area of the original healthy image and its transformed image. The background image is obtained

TABLE I. DETAILS OF CUCUMBER DATASETS

| Class | Train | Test |
|---|---|---|
| Healthy | 14,379 | 1,138 |
| Cucurbit chlorotic yellow virus (CCYV) | 4,721 | 1,248 |
| Melon yellow spot virus (MYSV) | 10,670 | 1,468 |
| Zucchini yellow mosaic virus (ZYMV) | 10,210 | 3,363 |
| Corynespora leaf sopt (CLS) | 6,675 | 491 |
| Powdery mildew (PM) | 6,390 | 1,135 |
| Total | 53,045 | 8,843 |

by the element-wise product of the input image and the leaf mask image (i.e., $x \odot (1 - S)$). Therefore,

$$\mathcal{L}_{\mathrm{bs}}(G, F) = \mathbb{E}_{x \sim p_{\mathrm{data}}(x)}\big[|(1 - S_x) \odot (G(x) - x)|_1\big] \\ + \mathbb{E}_{y \sim p_{\mathrm{data}}(y)}\big[|(1 - S_y) \odot (F(y) - y)|_1\big]. \quad (4)$$

Our final objective function is:

$$\mathcal{L}(G, F, D_X, D_Y) = \mathcal{L}_{\mathrm{adv}}(G, D_Y) + \mathcal{L}_{\mathrm{adv}}(F, D_X) \\ + \lambda\big[\mathcal{L}_{\mathrm{cyc}}(G, F) + \mathcal{L}_{\mathrm{bs}}(G, F)\big], \quad (5)$$

where $\lambda$ is a coefficient that determines the balance of loss term, and we set $\lambda = 10$ as in the original manuscript.

## III. Experiments

### A. Dataset

Table I shows the dataset used in this study. These are cucumber leaf images were taken under strict disease control at agricultural experiment stations in six Japanese prefectures between 2016 and 2020; each image shows a single leaf and has a diverse background. Our data differs from many other previous studies in that the training and test images were taken in different locations and are strictly differentiated. These are classified as three viral diseases (cucurbit chlorotic yellows virus: CCYV, melon yellow spot virus: MYSV, zucchini yellow mosaic virus: ZYMV), and two fungal diseases (corynespora leaf spot: CLS, powdery mildew: PM) or healthy.

### B. Training the bulk production phase

We collected in a total of 14,379 in-field healthy images in each of which has a size of $512 \times 512$ pixels for training the model. Our healthy generation model's input is a 512-dimensional random vector which was generated from a standard normal distribution, and the output is an image with the size of $512 \times 512$ pixels. We followed the best configuration as used in styleGAN2 [28] (i.e., config-f) to train our model. The Adam optimizer [30] and the minibatch size of 32 were applied. The training was finished after 600 epochs. For more details of training, please refer to the original paper.

### C. Training the pathogenic phase

Disease transformation models based on LeafGAN were trained to generate five types of diseases from healthy images. The training dataset for each transformation model is the number of healthy and disease images in the train set, as shown in Table I. The training of disease transformation
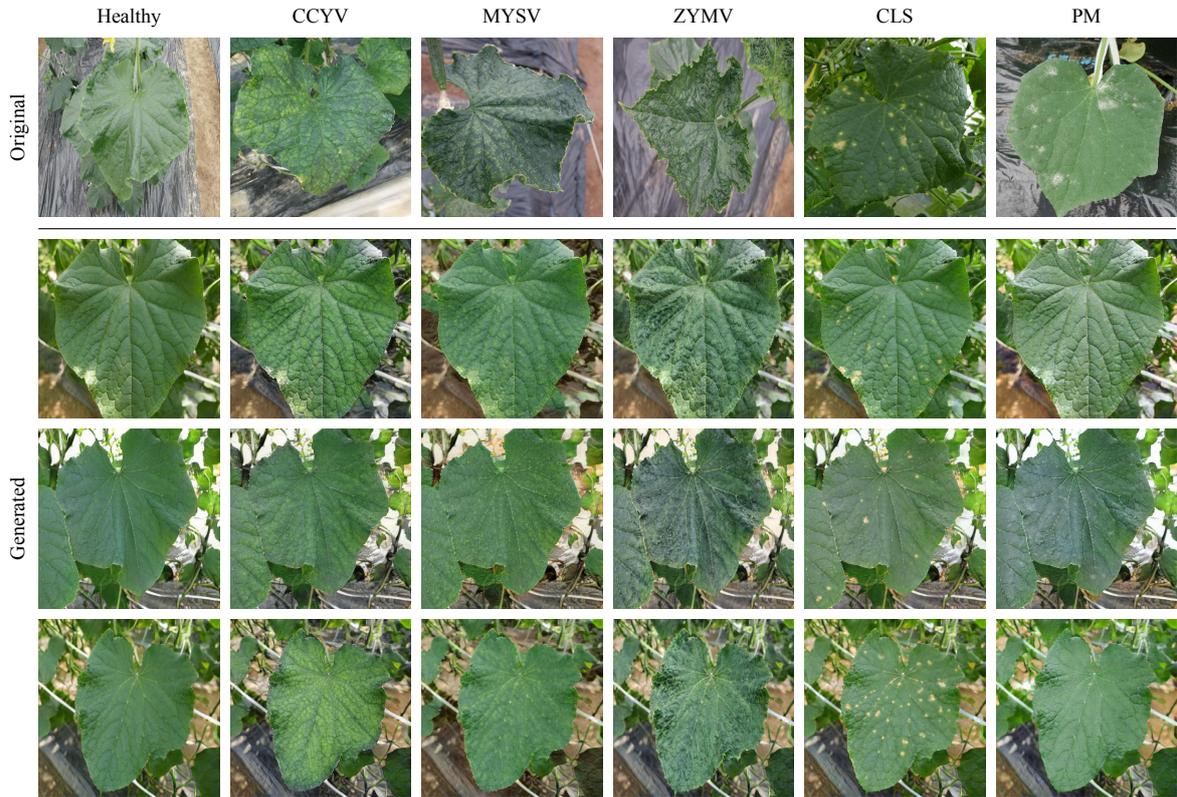
Fig. 2. Original (top row) and generated leaf images (the rows below). In generated images, the leftmost column shows the pseudo-healthy images generated in the bulk production phase. The remainder are pseudo-diseased images generated from pseudo-healthy images with added disease symptoms in the pathogenic phase.
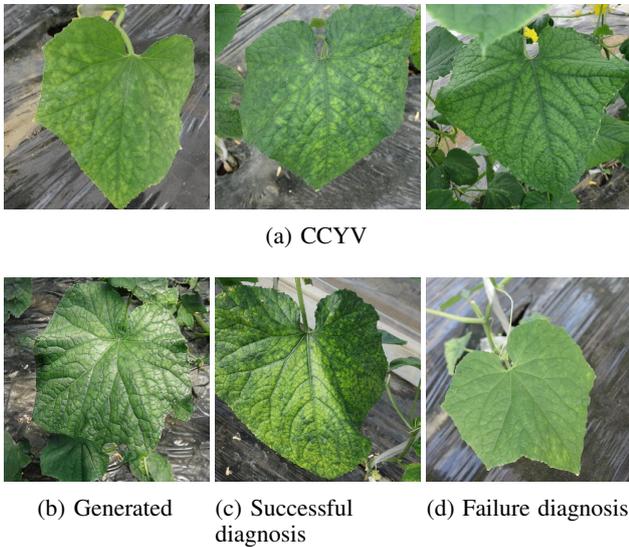


Fig. 3. (a): Examples of original CCYV images. (b): An example of generated CCYV image. (c) and (d): Examples of original CCYV test image which was classified correctly and not by the classifier trained with a dataset augmented by PPIG ($\times 2$).

models in the pathogenic phase was finished after 100 epochs. For more details of training, please refer to the LeafGAN paper [27]. For comparison, we also used the same dataset to train five CycleGAN disease transformation models with the same condition.

### D. Training disease classifiers

The effectiveness of the generated images as DA is evaluated using the diagnostic performance of the diseases. EfficientNet-B1 [31] was used for the plant disease classification models, and the input image size was set to $512 \times 512$ pixels. RandAugment [32] was used as the basic DA with parameters $N = 6$ and $M = 8$ based on the results of preliminary experiments. When training the classifiers, MomentumSGD [33] was used as the optimization method, $5 \times 10^{-5}$ for the training rate, $1 \times 10^{-4}$ for weight decay, and 0.9 for the coefficient of the momentum term. The F1-score and micro and macro averages for each class were used as evaluation indicators.

With each training data in Table I, the generated images were added to the original train dataset to create augmented datasets when training the model. In this study, we trained the following four disease classifiers.

- **Baseline**: Baseline with the EffictientNet-B1 [31] model is used. We trained this model for classifying six classes

TABLE II. DIAGNOSIS PERFORMANCE WITH AND WITHOUT GAN AUGMENTATION

| Method | F1-score [%] | | | | | | | |
|---|---|---|---|---|---|---|---|---|
| | Healthy | CCYV | MYSV | ZYMV | CLS | PM | Macro avg. | Micro avg. |
| Baseline | 65.3 | 76.9 | 62.1 | 82.5 | 52.9 | 59.2 | 66.5 | 71.5 |
| + CycleGAN | 65.1 | 77.7 | 64.0 | 86.2 | 53.8 | 66.4 | 68.9 | 74.3 |
| + Pathogenic phase | 67.1 | **79.9** | 64.4 | 84.5 | **59.4** | 73.4 | 71.4 | 75.4 |
| **(Proposed) + PPIG** (×2) | 75.1 | 75.3 | **73.2** | 92.5 | 59.3 | **79.9** | **75.9** | **81.2** |
| **(Proposed) + PPIG** (×3) | **76.0** | 76.3 | 72.2 | **92.7** | 55.5 | 79.5 | 75.4 | 81.1 |
| **(Proposed) + PPIG** (×4) | 75.9 | 75.1 | 71.9 | 92.3 | 57.1 | 79.8 | 75.3 | 80.8 |

(five diseases; one healthy) of the original dataset from Table I.

- **+CycleGAN** [24]: Same as the baseline model but trained with additional disease images generated by CycleGAN. For each disease class, we transformed new disease images from the original healthy data and added them to train set, and the number of images for each class was 14,379 (number of data in the largest class).

- **+Pathogenic phase**: Same as the baseline model but trained with additional data generated from the disease transformation model of the pathogenic phase. Each disease class has also been trained with extra generated images from healthy data, and the number of images for each class was 14,379. Note that this is comparable to LeafGAN, in which leaf region extraction was replaced to AOP.

- **(Proposal) +PPIG**: The proposed method of this study, PPIG, was used to generate healthy and diseased leaves. We used those generated images whose numbers are multiples of 14,379 for each class as the training data and evaluate the effect of training amount to the diagnostic performance.

Thanks to the production phase of the proposed PPIG, more images can be generated than the original number of data and can be added the training.

## IV. RESULT & DISCUSSION

### A. Visual evaluation of generated images

Fig. 2 shows original (top row) and generated leaf images (the rows below). In generated images, the leftmost column shows the pseudo-healthy images generated by styleGAN2 in the bulk production phase. The remainder are pseudo-diseased images generated from pseudo-healthy images with added disease symptoms in the pathogenic phase.

Although some of the generated images had unnatural background areas, the shapes and the veins of the leaves were reproduced as well as the original images. For the generated images of the diseased leaves, we can confirm that the background changes are suppressed, and appropriate changes are made in the leaf region.

### B. Evaluation of DA by generated images

Table II shows a comparison of the disease classification performance in each scenario. Baseline's F1-score was 66.5%

on macro average, but augmentation, which doubles the number of images generated by the proposed PPIG, improved the performance by 9.4% to 75.9%. This result is 4.5% better than DA without the bulk production phase and is 7.0% better than DA with CycleGAN. Similar to the results of the micro average, our PPIG is also able to achieve 81.2% with a 9.7% improvement in performance over the Baseline. Therefore, it is considered that the classifier successfully learned more variety of distribution expanded by PPIG than the original images and became robust in classifying data from different fields. In addition, the constraint of background change in the pathogenic phase was effective because the pathogenic phase increases the score of the CycleGAN. The DA effect of PPIG was highest when the number of images was doubled in the range of experiments, with a slight decrease when the number of images was increased by a factor of three or four. The reason for this is that the diversity of the generated images is bounded by the distribution of the original images estimated by the bulk production phase. Thus, classifiers have started to learn similar generated images.

On the other hand, unlike the other four diseases and health, CCYV was only as accurate as the baseline, with no DA effect. Fig. 3 shows typical examples of original CCYV images, CCYV images generated by PPIG and test images of CCYV that are correctly or mistakenly identified by the classifier trained by the PPIG (×2) dataset. Texture shading, which is a symptom of CCYV, appears clearly in the generated image. The image was classified correctly; however, the symptom does not appear strongly in the image classified wrong. Since many of the generated images show strong symptoms, the classifier learned by adding them to the images may be more likely to misidentify weak symptoms, such as early symptoms. We believe that adjusting the strength of the addition of symptoms leads to room for improvement in the future.

## V. CONCLUSION

In this study, we proposed a productive and pathogenic image generation (PPIG), a framework for generating varied and quality plant images, and showed that it effectively improves the cucumber disease diagnostic performance. It was shown that expanding the training dataset by generating more number of healthy leaf images and transforming them into disease images can enhance the classifier's ability over the recently reported GAN-based DA methods. We confirmed the

effectiveness of the proposed framework as a DA for automatic disease diagnosis based on leaves.

## ACKNOWLEDGMENT

## REFERENCES

[1] FAO, "Protecting plants, protecting life," *Food and Agriculture Organization of the United Nations*, 2020. [Online]. Available: http://www.fao.org/plant-health-2020/about/en/

[2] Y. Kawasaki, H. Uga, S. Kagiwada, and H. Iyatomi, "Basic study of automated diagnosis of viral plant diseases using convolutional neural networks," *International Symposium on Visual Computing*, pp. 638–645, 2015.

[3] H. David and S. Marcel, "An open access repository of images on plant health to enable the development of mobile disease diagnostics," *CoRR arXiv:1511.08060*, 2015.

[4] S. P. Mohanty, D. P. Hughes, and M. Salathé, "Using deep learning for image-based plant disease detection," *Frontiers in plant science*, vol. 7, p. 1419, 2016.

[5] G. Wang, Y. Sun, and J. Wang, "Automatic image-based plant disease severity estimation using deep learning," *Computational Intelligence and Neuroscience*, vol. 2017, 2017.

[6] H. Durmuş, E. O. Güneş, and M. Kırcı, "Disease detection on the leaves of the tomato plants by using deep learning," in *International Conference on Agro-Geoinformatics*. IEEE, 2017, pp. 1–5.

[7] H. A. Atabay, "Deep residual learning for tomato plant leaf disease identification," *Journal of Theoretical & Applied Information Technology*, vol. 95, no. 24, 2018.

[8] K. P. Ferentinos, "Deep learning models for plant disease detection and diagnosis," *Computers and Electronics in Agriculture*, vol. 145, pp. 311–318, 2018.

[9] V. K. Shrivastava, M. K. Pradhan, S. Minz, and M. P. Thakur, "Rice plant disease classification using transfer learning of deep convolutional neural network," *International Archives of the Photogrammetry, Remote Sensing & Spatial Information Sciences*, 2019.

[10] S. Ren, K. He, R. Girshick, and J. Sun, "Faster r-cnn: Towards real-time object detection with region proposal networks," *Advances in Neural Information Processing Systems*, pp. 91–99, 2015.

[11] W. Liu, D. Anguelov, D. Erhan, C. Szegedy, S. Reed, C.-Y. Fu, and A. C. Berg, "SSD: Single shot multibox detector," *European Conference on Computer Vision*, pp. 21–37, 2016.

[12] A. Fuentes, S. Yoon, S. C. Kim, and D. S. Park, "A robust deep-learning-based detector for real-time tomato plant diseases and pests recognition," *Sensors*, vol. 17, no. 9, p. 2022, 2017.

[13] H. Q. Cap, K. Suwa, E. Fujita, S. Kagiwada, H. Uga, and H. Iyatomi, "A deep learning approach for on-site plant leaf detection," *The IEEE International Colloquium on Signal Processing & Its Applications*, pp. 118–122, 2018.

[14] K. Suwa, Q. H. Cap, R. Kotani, H. Uga, S. Kagiwada, and H. Iyatomi, "A comparable study: Intrinsic difficulties of practical plant diagnosis from wide-angle images," *The IEEE International Conference on Big Data*, pp. 5195–5201, 2019.

[15] A. F. Fuentes, S. Yoon, J. Lee, and D. S. Park, "High-performance deep neural network-based tomato plant diseases and pests diagnosis system with refinement filter bank," *Frontiers in plant science*, vol. 9, p. 1162, 2018.

[16] T. Saikawa, Q. H. Cap, S. Kagiwada, H. Uga, and H. Iyatomi, "Aop: An anti-overfitting pretreatment for practical image-based plant diagnosis," pp. 5177–5182, 2019.

[17] E. Fujita, H. Uga, S. Kagiwada, and H. Iyatomi, "A practical plant diagnosis system for field leaf images and feature visualization," *International Journal of Engineering & Technology*, vol. 7, no. 4.11, pp. 49–54, 2018.

[18] I. Goodfellow, J. Pouget-Abadie, M. Mirza, B. Xu, D. Warde-Farley, S. Ozair, A. Courville, and Y. Bengio, "Generative adversarial nets," *Advances in Neural Information Processing Systems*, pp. 2672–2680, 2014.

[19] J. A. Pandian, G. Geetharamani, and B. Annette, "Data augmentation on plant leaf disease image dataset using image manipulation and deep learning techniques," *The IEEE International Conference on Advanced Computing*, pp. 199–204, 2019.

[20] Q. Zeng, X. Ma, B. Cheng, E. Zhou, and W. Pang, "Gans-based data augmentation for citrus disease severity detection using deep learning," *IEEE Access*, vol. 8, pp. 172 882–172 891, 2020.

[21] Q. Wu, Y. Chen, and J. Meng, "Dcgan based data augmentation for tomato leaf disease identification," *IEEE Access*, vol. 8, pp. 98 716–98 728, 2020.

[22] N. M. Nafi and W. H. Hsu, "Addressing class imbalance in image-based plant disease detection: Deep generative vs. sampling-based approaches," *International Conference on Systems, Signals and Image Processing*, pp. 243–248, 2020.

[23] A. Radford, L. Metz, and S. Chintala, "Unsupervised representation learning with deep convolutional generative adversarial networks," *International Conference on Learning Representations*, pp. 1–16, 2015.

[24] J.-Y. Zhu, T. Park, P. Isola, and A. A. Efros, "Unpaired image-to-image translation using cycle-consistent adversarial networks," *The IEEE International Conference on Computer Vision*, pp. 2223–2232, 2017.

[25] Y. Tian, G. Yang, Z. Wang, E. Li, and Z. Liang, "Detection of apple lesions in orchards based on deep learning methods of cyclegan and yolov3-dense," *Journal of Sensors*, vol. 2019, 2019.

[26] H. Nazki, S. Yoon, A. Fuentes, and D. S. Park, "Unsupervised image translation using adversarial networks for improved plant disease recognition," *Computers and Electronics in Agriculture*, vol. 168, pp. 105–117, 2020.

[27] Q. H. Cap, H. Uga, S. Kagiwada, and H. Iyatomi, "Leafgan: An effective data augmentation method for practical plant disease diagnosis," *CoRR arXiv:2002.10100*, 2020.

[28] T. Karras, S. Laine, M. Aittala, J. Hellsten, J. Lehtinen, and T. Aila, "Analyzing and improving the image quality of stylegan," *The IEEE Conference on Computer Vision and Pattern Recognition*, pp. 8110–8119, 2020.

[29] P. Isola, J.-Y. Zhu, T. Zhou, and A. A. Efros, "Image-to-image translation with conditional adversarial networks," *The IEEE Conference on Computer Vision and Pattern Recognition*, pp. 1125–1134, 2017.

[30] D. P. Kingma and J. Ba, "Adam: A method for stochastic optimization," *CoRR arXiv:1412.6980*, 2014.

[31] M. Tan and Q. Le, "Efficientnet: Rethinking model scaling for convolutional neural networks," *International Conference on Machine Learning*, pp. 6105–6114, 2019.

[32] E. D. Cubuk, B. Zoph, J. Shlens, and Q. V. Le, "Randaugment: Practical automated data augmentation with a reduced search space," pp. 702–703, 2020.

[33] N. Qian, "On the momentum term in gradient descent learning algorithms," *Neural Networks*, vol. 12, no. 1, pp. 145–151, 1999.